

### C-1.1.1 Research on the transport/transformation model for environmental acidification and the integration of the atmosphere-soil model.

**Contact person** Kentaro Murano  
Department of Global Environment Research  
National Institute for Environmental Studies  
Onogawa 16-2, Tsukuba, Ibaraki 305-0053, Japan  
Tel. +81-298-50-2537 Fax +81-298-50-4732  
E-mail: murano@nies.go.jp

**Total Budget of FY1996-FY1998** 53,718,000 Yen (FY1998; 15,079,000 Yen)

**Abstract** A long-range transport model including a detailed chemical reactions was applied to characterize the transboundary pollutant transport during both wintert and the Baiu season, and model results were compared with the aerosol high concentration observed in Tsushima, Chikugo-Ogori and Seoul in June 1991 and February 1992. Long-range transport model results and backward trajectory analysis indicate that mesoscale phenomena such as synoptic scale high/low pressure change and the Baiu rainfront located between the southern part of China and the south of Japan island plays an important role for transportation the air pollutant emitted from China and Korean peninsula and for its transport/transformation to the northern Kyushu area. It was revealed that the north-south movement of Baiu rainfront is significantly important for the aerosol high concentration over the Kyushu and western part of Japan area.

**Key Words** Long-range transport model, Sulfate, Nitrate, deposition, Baiu front

#### 1. Introduction

Acid deposition is widely recognized as one of the most serious global atmospheric pollution problems. East Asian countries face a potential regional scale, international acid deposition problem, and have recently started to expand their monitoring activities.

It is pointed out that wind pattern variations associated with synoptic scale pressure system changes are extremely important for the transboundary transport of pollutants (Uno *et al.*, 1997a). To understand the long-range transport phenomena, series of special aerosol observations (surface and airborne) have been conducted during the winter monsoon because high concentration of SO<sub>2</sub> and sulfate are usually observed.

Recently, Mori *et al.* (1997) and Waka-matsu *et al.* (1996) revealed that the aerosol concentration level is also high during the early summer rainy season (in Japan, it sets in early June and over in the middle of July). This rainy season is characterized by an existence of a west-east oriented beltlike precipitation region (rainy meso-front), whose latitudinal location is primarily determined by interaction between the Pacific subtropical high and continental / Okhotsk high. Because direct contributors to rainfall amount consist of synoptic and mesoscale systems such as fronts, low-level jets, and vortices, so the distribution of rainfall amount in the belt is non-uniform and the location of this rainbelt zone oscillates south-north direction due to the relative strength of the Pacific and continental high pressure system. It is important to notice that air mass under the Pacific high pressure system is relatively clean while the air mass under the continental high is usually polluted due to the existence of the intense pollutants emission area. In this paper, long-range transport simulation results during the early summer rainy season by STEM-II (Carmichael *et al.*, 1986) is reported.

## 2. Observation and STEM results

### 2.1 Synoptic Weather Pattern and Observation Data in June 1991

The field observation details and the results of a basic analysis of the observed aerosol data have already been reported in Wakamatsu *et al.* (1996) and Mori *et al.* (1997). In this observation, aerosols were collected at three locations in Japan and Korea - two urban sites (Ogori in Fukuoka prefecture, Japan and Seoul, Korea) and one rural site (Tsushima in Nagasaki prefecture, Japan) shown in Figure 1. Aerosol samples were collected over periods of one to two weeks every two months from August 1990 to February 1992 (with four or eight hour intervals). The high average concentrations of  $\text{NO}_3^-$ ,  $\text{SO}_4^{2-}$ ,  $\text{Ca}^{2+}$  and  $\text{Mg}^{2+}$  were detected in June 1991. The observation in June 1991 was conducted during the meteorological condition for typical rainy season.

The rainy meso-front stayed near the south edge of the Japan Islands from the beginning of June, and the wind convergence zone was observed along the meso-front lines. The wind speed of the northern part of this meso-front was relatively small and the air was stagnant. Precipitation was recorded on the 12th, 13th, 15th, 19-20th and 25-26th, June 1991 at Tsushima (Heavy rain of 44 mm was recorded on the 13th. Except for this heavy rain, total precipitation was 14 mm).

Figure 2 shows the location of rainy meso-front and the isentropic backward trajectories calculated from Tsushima from June 11 to 28, 1991 at 1500 m level. It is very clear that the existence of a west-east oriented rainy meso-front and a beltlike precipitation region ( $25^\circ \text{N} \sim 35^\circ \text{N}$ ) divided the atmosphere between the Pacific maritime airmass and continental/ Okhotsk airmass. Trajectory paths can be classified into two categories, that is, the transport from maritime airmass and the continental air mass which has very stagnant characteristics between the north of Kyushu, Japan and the Korean peninsula.

Figure 3 show the time variation of (a) hourly precipitation at Tsushima and (b)-(d)  $\text{SO}_4^{2-}$  observed in three observation sites, respectively (Open circles in figure shows the observation), and the STEM results (legends in figure indicate the heterogeneous reaction rate experiments discussed later). Arrows in figures indicates the wind speed and horizontal direction at  $z=1000$  m.

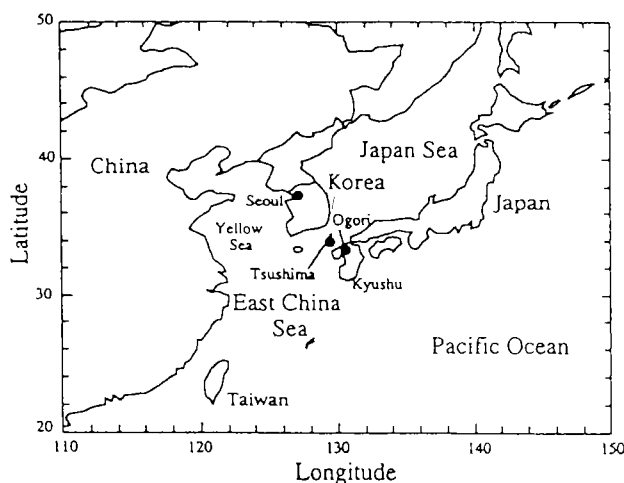


Fig. 1 Location of observation sites and STEM calculation domain.

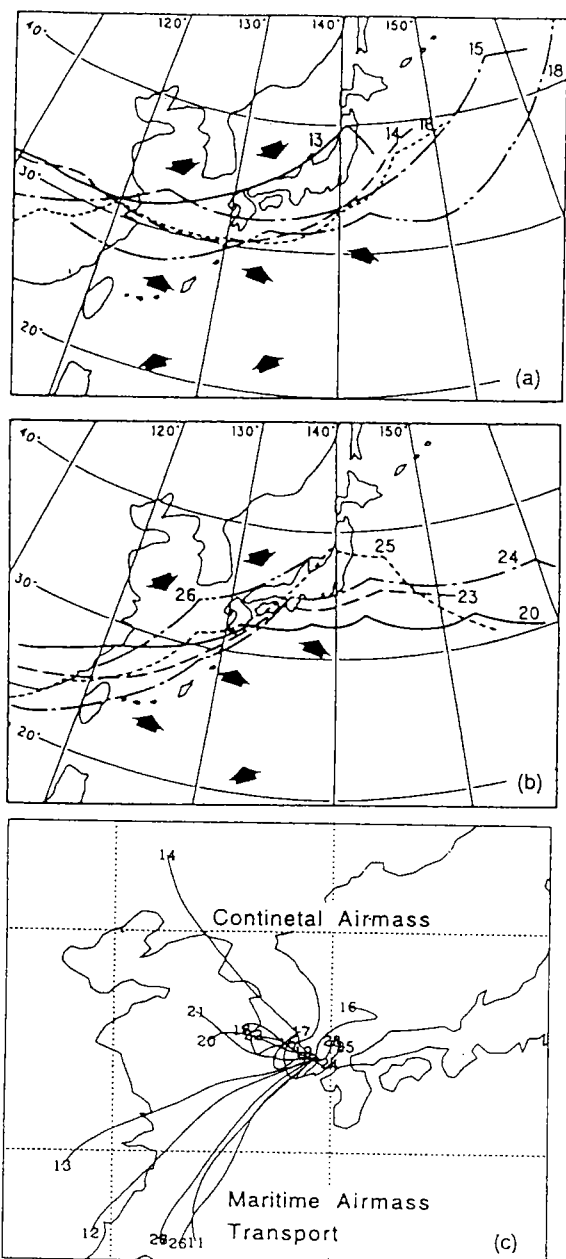


Fig. 2 (a) Location of rainy meso-front at June, 13, 14, 15, 16 and 18, 1991 (b) location of rainy meso-front at June, 20, 23, 24, 25 and 26, 1991 (c) isentropic backward trajectories calculated from Tsushima at  $z=1500\text{m}$  for 36 hours. Number in figure indicates the backward trajectory starting date.

## 2.2 Numerical configuration of STEM

To understand the observed characteristics of long-range transport of pollutants, an atmospheric transport model which includes detailed chemical reactions, the STEM-II (Carmichael *et al*, 1986), was applied. STEM-II is a three-dimensional Eulerian numerical model which accounts for transport, chemical conversion, and deposition of atmospheric pollutants. The major features of STEM-II include: emission of pollutants from point and area sources; transport by advection, convection, and turbulent diffusion; and spatially and temporally varying wind,

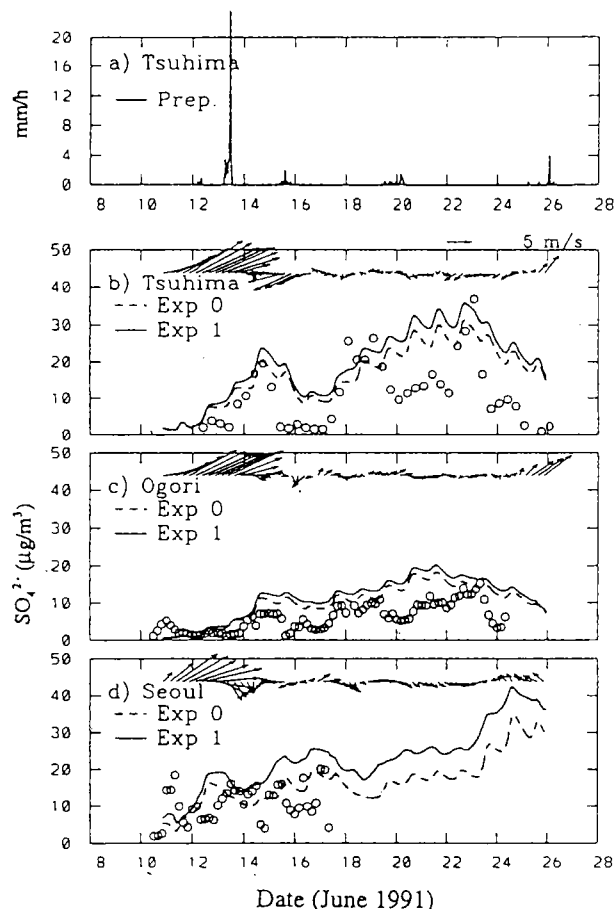


Fig. 3 (a) Time variation of hourly precipitation observed at Tsushima. Time variation of observed (open circle) and numerical values (bold line for Exp. 1; broken line for Exp. 0) for  $\text{SO}_4^{2-}$  at (b) Tsushima, (c) Ogori, (d) Seoul. Arrows in figures indicate the wind vector and direction at  $z=1000\text{m}$ .

temperature, pressure, water vapor, precipitation, and cloud fields. A detailed description of STEM-II can be found in Carmichael *et al.* (1986).

In the present application, no precipitation or cloud processes were considered. The East Asia model domain was a  $1^\circ$  latitude x  $1^\circ$  longitude grid system. The model domain covers from  $110^\circ$  E to  $150^\circ$  E and  $20^\circ$  N to  $50^\circ$  N. This horizontal domain is divided into a 41 x 31 mesh. The vertical model domain consists of 10 layers from ground level to 10,000 m. The vertical grid levels are 200, 400, 700, 1000, 2000, 3000, 4000, 5000, 7000, 10000 m. Global analysis meteorological data (GANL) by Japan Meteorological Agency (JMA) are used for wind field data.

STEM numerical calculations were started with zero initial values except for  $O_3$  (which was set 35 ppb throughout the calculation domain). Simulated atmospheric aerosol concentrations were then compared with the intensive measurement data. It is important to point out that the present model results are compared with short time interval measurements of atmospheric aerosol concentrations.

Experiments were conducted by changing the pre-assigned heterogeneous reaction rate ( $SO_2$ -gas  $\rightarrow$   $SO_4^{2-}$ -aerosol) from 0.0 %/h (Exp. 0) to 1.0 %/h (Exp. 1).

### 2.3 Results of STEM application

Figure 3 compares model simulation  $SO_4^{2-}$  results (dashed line = 0%/h, straight line = 1%/h heterogeneous reaction rate) and observation data (open symbol) at Tsushima, Ogori and Seoul. Model concentrations in the first vertical level were used in this plot.

Figure 4 shows horizontal wind vector, the calculated distribution of  $SO_4^{2-}$  (contour in  $\mu\text{g}/\text{m}^3$ ) and conversion factor,  $F_s$  (tone) at  $z^*=200$  m level on June 14, 16, 22 and 25 1991. Here,  $F_s$  is defined by

$$F_s = \frac{SO_4^{2-}[S]}{SO_2[S] + SO_4^{2-}[S]} \quad (1)$$

Figure 3 indicates that the STEM calculation successfully simulated the typical time variation of observed  $SO_4^{2-}$  concentrations. However, the model generally well predicted sulfate concentration levels, some of periods are higher than observation (overprediction was obvious from the 20th to 22th as can be seen in Figure 3). One highly plausible interpretation of this overprediction is the fact that the present model application ignores wet removal processes.

It is clear from Figure 4 that the rainy meso-front line plays an important role in the trans-boundary transport of pollutants. A high pollutant concentration region was simulated in the eastern part of China and southeast part of Korean peninsula, these polluted regions are mostly located at the northern part of rainy meso-front region. It is also important to point out that there are very sharp concentration gradients between Kyushu, Japan and the southern part of the Korean peninsula (Figure 4). Horizontal diffusivity in model and this strong concentration gradient are another reason of concentration level overprediction at Tsushima and Ogori.

The calculated concentrations at Tsushi-ma decrease after June 24 because the rainy meso-front moved from the southern edge of the Japan Islands to the southern part of Korean peninsula and these area is covered by the maritime clean air.

Difference in simulated  $SO_4^{2-}$  between the heterogeneous reaction rate of 0%/h and 1%/h is small in Tsushima and Ogori. This fact indicates that the gas phase reaction played an important role at the northern part of rainy meso-front because the air is very stagnant at there, and most of  $SO_2$  was already converted to  $SO_4^{2-}$ .

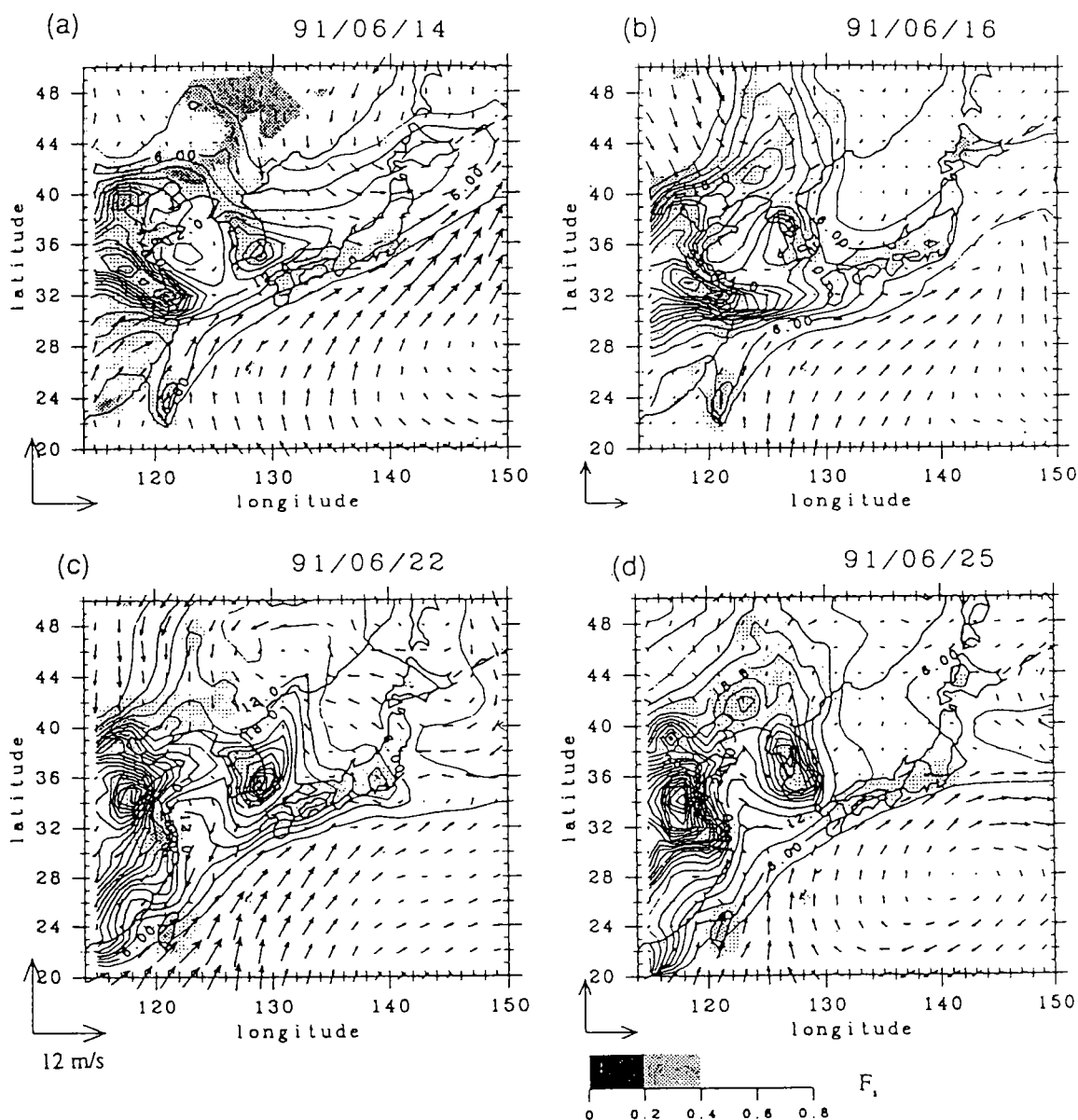


Fig. 4 Wind vector,  $\text{SO}_4^{2-}$  (contour; contour interval is  $3\mu\text{g}/\text{m}^3$ ) and sulfate conversion factor  $F_s$  (tone) from Exp. 1 at  $z=200\text{m}$ . Wind scale indicates wind speed of 12 m/s. (a) June 14, 1991, (b) June 16, 1991, (c) June 22, 1991, (d) June 25, 1991.

Present numerical study ignored the precipitation or cloud processes in transport and chemical reactions even if the STEM has the proper module to handling these processes. This is because the reliable high resolution cloud and precipitation distribution was not available. To overcome these problems, new numerical approach based on the RAMS will be discussed in the following section to the same episode.

### 3. Summary

High aerosol concentration level was observed within an early summer rainy season (June 1991) in Japan. West-east oriented rainy meso-front line (rainbelt located at  $25^\circ\text{N}\sim 35^\circ\text{N}$ ) characterizes the rainy season and divides the atmosphere between the less polluted Pacific maritime airmass and polluted continental airmass.

To understand a long-range transport phenomena during this season, STEM-II are applied. STEM results explained well the concentration variation, and indicates that the strong concentration gradients exists at the northern side of rainy meso-front (typically at Korea and Kyushu Japan). It was found that the location of rainy meso-front plays an important role for sulfate concentration level in Japan and Korea. Numerical results also indicates the importance of wet removal processes near rainy meso-front region.

### References

- Akimoto H. and Narita H., 1994: Distribution of SO<sub>2</sub>, NO<sub>x</sub> and CO<sub>2</sub> emissions from fuel combustion and industrial activities in Asia with 1° x 1° resolution, *Atmos. Environ.*, **28**, 213-225.
- Carmichael G.R., Peters L.K. and Kitada T., 1986: A second generation model for regional-scale transport/ chemistry/ deposition, *Atmos. Environ.*, **20**, 173-188.
- Mori, A., A. Utsunomiya, I. Uno, S. Waka-matsu and T. Ohara, 1997: Analysis of aerosol concentration variation and high concentration episodes observed in the northern Kyushu area, *J. Japan Atmos. Environ.*, **32**, 73-89 (in Japanese).
- Uno, I. T. Ohara and K. Murano, 1997a: Simulated acidic aerosol long-range transport and deposition over east Asia - role of synoptic scale weather systems, *22nd NATO/CCMS International Technical Meeting on Air Pollution Modeling and its Application*, 119-126, June, France.
- Uno, I., T. Ohara, A. Mori, A. Utsunomiya, S. Wakamatsu and K. Murano, 1997b: Numerical analysis of long-range transport and transformation over the East Asia, *J. Japan Atmos. Environ.*, **32**, 267-285. (in Japanese)
- Wakamatsu, S., A. Utsunomiya, J.-S. Han, A. Mori, I. Uno and K. Uehara, 1996: Seasonal variation in atmospheric aerosol concentration covering northern Kyushu, Japan and Seoul, Korea, *Atmos. Environ.*, **30**, 2343-2354.
- Wesely, M.L., 1988: Improved parameterizations for surfaces resistance to gaseous dry deposition in regional scale model, *EPA/6003-86/037* (PB86-218104).